GRANULOMETRIC ANALYSIS OF PALEOTSUNAMI DEPOSITS CANDIDATE IN TERNATE ISLAND, NORTH MALUKU

ANALISIS GRANULOMETRIK TERHADAP KANDIDAT ENDAPAN TSUNAMI DI PULAU TERNATE, MALUKU UTARA

Yudhicara*

Center for Volcanology and Geological Hazard Mitigation – Geological Agency Jl. Diponegoro 57 Bandung, Indonesia

*Corresponding author: yudhicara966@gmail.com

(Received 30 January 2023; in revised from 3 February 2023; accepted 25 July 2023)

DOI : http://dx.doi.org/10.32693/bomg.38.2.2023.807

ABSTRACT: Ternate Island is a volcanic island located in the Maluku Sea. Tsunami ever hit Ternate before 1900 or occurred before the age of the people living in this island. The paleotsunami suspect have been found in the western coast of Ternate Island. The outcrop has 50 m length and 1 m width, was discovered beneath the Gamalama eruption product which occurred in 1907. The paleotsunami candidate consists of at least five layers originating from different tsunami events. The granulometric analysis was carried out for each layer. The results obtained were that paleotsunami sediments had poorly sorted which indicated that the grain sizes were mixed, this was due to the energy of tsunami wave varied in time when transporting and depositing the sediments. Skewness varies from very fine to very coarse, indicating a change in the energy of the tsunami wave that occurs from very high when rising inland to decreasing as it returns to sea. Kurtosis varies from leptokurtic, platykurtic, and mesokurtic. Variations in mean, sorting, skewness and kurtosis values indicate a change in tsunami wave energy which causes a change in grain size. The granulometric analysis shows that the deposition of the youngest paleotsunami deposits candidate was initiated by a very strong current with the greatest energy, thus depositing very coarse sand to gravel, followed by a gradual decrease in energy and the tsunami wave process began to reverse towards the sea, then receded with the lowest energy and deposited finer grains. The sediment sources come from two different places, this shows that the sources come from the sea and the coast around the deposited paleotsunami candidates.

Keywords: paleotsunami deposits, deposition process, granulometric analysis, Ternate, North Maluku

ABSTRAK: *Pulau Ternate merupakan pulau gunung api yang terletak di Laut Maluku. Tsunami pernah melanda Ternate sebelum tahun 1900 atau terjadi sebelum usia penduduk yang tinggal di pulau ini. Kandidat paleotsunami telah ditemukan di pesisir barat Pulau Ternate. Singkapan tersebut memiliki panjang 50 m dan lebar 1 m, ditemukan di bawah produk letusan Gamalama yang terjadi pada tahun 1907. Kandidat paleotsunami terdiri dari paling tidak, lima lapisan yang berasal dari peristiwa tsunami yang berbeda. Analisis granulometri telah dilakukan untuk masing-masing lapisan. Hasil yang diperoleh bahwa endapan paleotsunami memiliki sortasi yang kurang baik yang mengindikasikan bahwa ukuran butir tercampur, hal ini disebabkan energi gelombang tsunami bervariasi terhadap waktu saat mengangkut dan mengendapkan sedimen. Skewness bervariasi dari sangat halus hingga sangat kasar, menunjukkan perubahan energi gelombang tsunami yang berlaku dari sangat tinggi ketika naik ke daratan menurun ketika kembali ke laut. Kurtosis bervariasi dari leptokurtik, platikurtik, dan mesokurtik. Variasi nilai mean, sorting, skewness dan kurtosis menunjukkan adanya perubahan energi gelombang tsunami yang menyebabkan perubahan ukuran butir. Analisis granulometrik menunjukkan bahwa endapan yang diduga produk paleotsunami termuda, proses pengendapannya diawali oleh arus yang sangat kuat dengan energi terbesar, sehingga mengendapkan pasir yang sangat kasar hingga kerikil, diikuti dengan penurunan energi secara bertahap dan proses gelombang tsunami mulai berbalik arah menuju laut, kemudian surut dengan energi terendah dan mengendapkan butir-butir yang lebih halus. Sumber sedimen tersebut berasal dari dua tempat yang berbeda, yaitu berasal dari laut dan pantai di sekitar endapan yang diduga hasil kejadian tsunami masa lalu (paleotsunami).*

Kata Kunci: *endapan paleotsunami, proses pengendapan, analisis granulometri, Ternate, Maluku Utara*

INTRODUCTION

Ternate Island is a volcanic island located in the Maluku Sea. Based on its tectonic conditions, Ternate is an area prone to tsunamis, which caused by earthquakes, volcanic activity or due to underwater landslides. According to the tsunami catalog, tsunami have ever hit Ternate Island in 1608, 1673, 1771, 1840, 1846, 1856, 1857, 1858, 1859, 1871, 1889, 1892, 1900 (Soloviev & Ch.N.Go., 1974), and 1994 (Satake & Imamura, 1995).

The tsunami history in this island was occurred before the age of the people living in this island. Therefore, the tsunami traces findings on this island can be very important as an early warning to the people to face the similar tsunami events that might occur in the future.

The Maluku Sea is an arc-arc collision zone, which is located at the confluence of the Eurasian, Pacific and Philippine plates (Figure 1). This collision forms a double subduction zone in the Maluku Sea known as the Mayu Ridge subduction zone.

The consequences of this subduction zone produce a series of volcanoes along the west in the Sangihe Islands and in the east along Halmahera Island and form volcanic islands, which is Ternate is one of them and Gamalama is the name of the volcano.

In the investigation of tsunami traces in Ternate Island which conducted on November 2022, at least three paleotsunami layers have been found in the western part of the Island, namely the Loto area (Figure 2). The Loto area has characteristics of a straight beach with a wavy morphology, composed of sand, gravels, pebbles to boulder of rocks which are products of the Gamalama volcano.

Based on its position, Loto is located in an estuary, the mouth of the Loto river or also known as Barangka Loto (Barangka means river) which ends into the Maluku Sea. This place relatively natural and undisturbed by human activity.

Based on the Geological Map of Gamalama Volcano, Ternate, North Maluku, surface deposits of Ternate Island are composed by the results of eruptions from the Gamalama Volcano itself (Figure 3). Starting from Prehistoric times (before the 5th century) to the present (Bronto et al., 1982).

The deposits of each generation of the Gamalama volcano, based on the source of the eruption, are divided into three parts, in order from oldest to youngest, as follows: Old Gamalama (Gt) consists of types of lava flows and related rocks (GtLu); Pyroclastic deposits (Gtig); and the lava deposit (GtLa), occurred in Pre-historic times. Mature Gamalama (Gd) consists of types of lava flows and related rocks, namely GdL and GdLu; Pyroclastic deposits consist of Gdpf, Gdpl, Gdp; and the Gdla lava deposits. Happened in pre-historic times.

Young Gamalama (Gm) which is divided into two based on the time it occurred, namely the prehistoric era and the historical era. In prehistoric times, it consisted of related types of lava flows and rocks, namely GmLu, Gm L1, Gm L2, Gm L3, and Gm L5, while those that occurred in historical times were Gm L6, and Gm L7. Whereas pyroclastic deposit products in prehistoric times consisted of Gm pf, and those that occurred in historical times were Gmbv and Gmpm, and Gmpt which lasted from

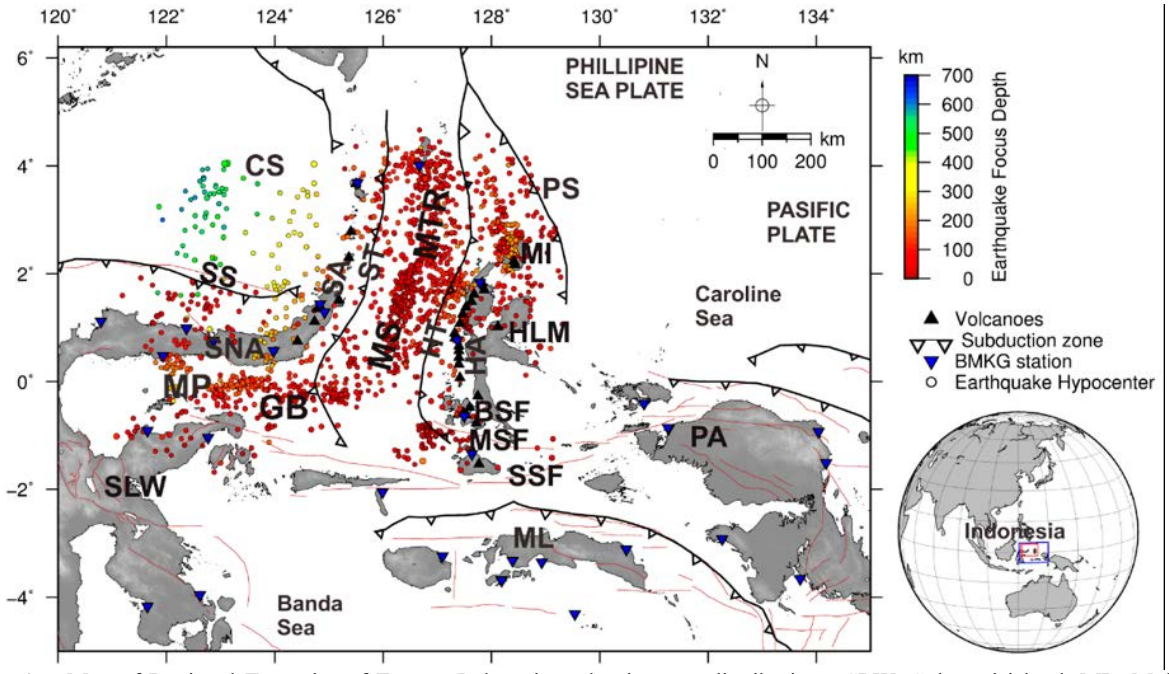

Figure 1. Map of Regional Tectonics of Eastern Indonesia and epicenters distributions; SLW: Sulawesi island; ML: Molucca island; PA: Papua island; HLM: Halmahera island; SNA: Sulawesi's north arm; SS: Sulawesi slab; PS: Philippine slab; HT and ST: Halmahand Sangihe Trench; HA and SA: Halmahera and Sangihe volcanoes arc; CS: Celebes sea; MP: Minahassa peninsula; GB: Gorontalo Basin; MS: Molucca Sea; MTR: Mayu-Talaud Ridge; BSF, MSF, and SSF: Bacan, Molucca, and Sula Sorong Faults, respectively (Rachman et al., 2022).

Figure 2. Area of Interest (left) in the western part of Ternate (right) (Google Earth, 2022)

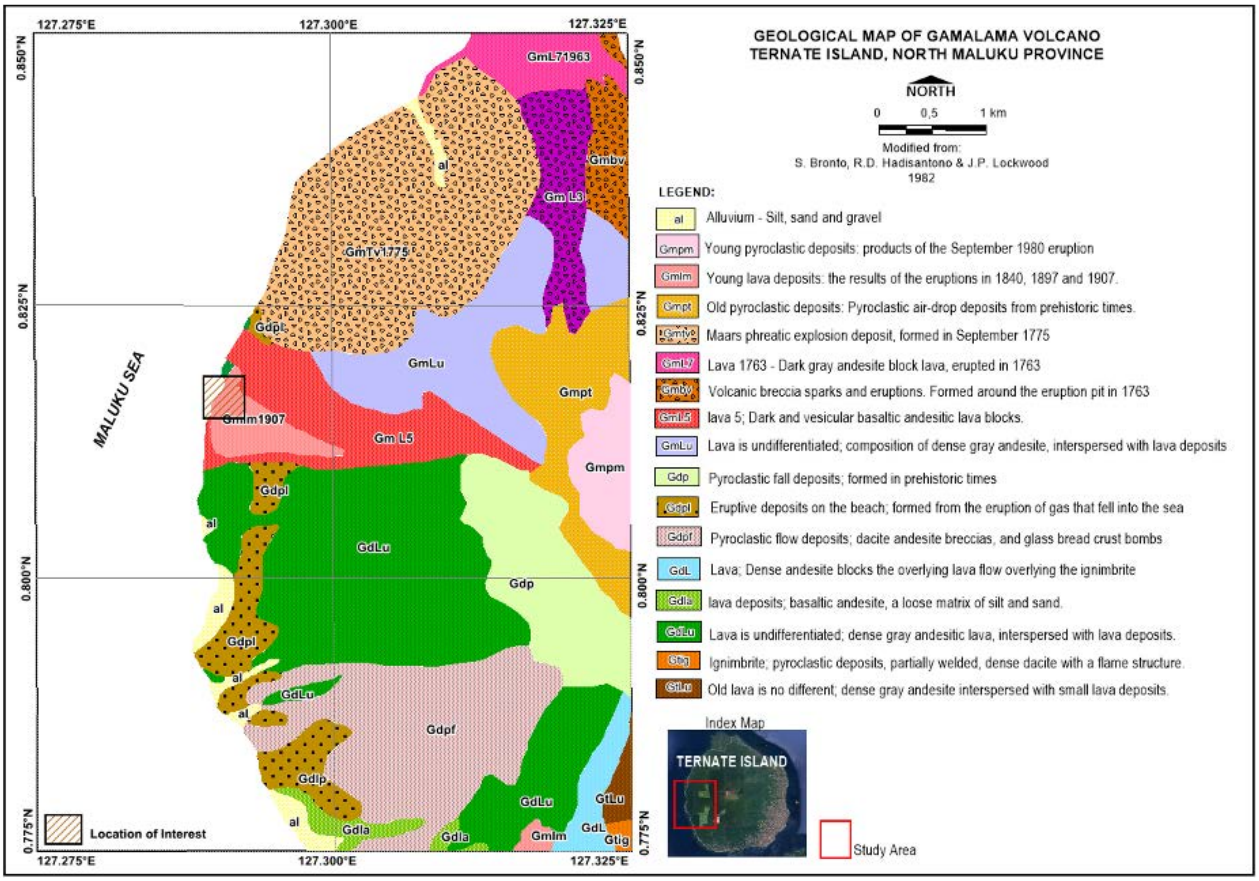

Figure 3. Geological Map of Gamalama Volcano (Bronto et al., 1982)

prehistoric times to historical times; There are Maar deposit products, which occurs as a result of weakly consolidated phreatic eruptions, while on the slopes as layered foundation deposits with bomb, sag and plant lapilli structures; whereas in historical times there were phreatic eruptions accompanied by the formation of the Tolire Jaha and Tolire Kecil maars, which occurred in 1775 (GmTv). Lava deposits occurred in historical times, namely Gmlm, which is a young lava deposit. Surface deposits consist of debris pyroclastic deposits (pr) and alluvium consisting of silt, sand, gravel and lumps (al).

Tsunami deposits are generally preserved in low-lying areas such as estuaries and lagoons and are made up of sediments resulting from the erosion of coastal areas (sand dunes, beach embankments, cliffs) and parts of the seabed that were eroded by the tsunami waves.

The tsunami deposits show a wide variety of bed forms and sedimentary structures; their properties are

highly dependent on the physical setting of the deposition site and on the nature of the events that caused it, such as current strength and surface geology. However, some common features are recognized in most tsunami deposits, reflecting the physical nature of the tsunami waves. Very large wavelength and period compared to storm surge. At the same time, these general features reflecting the shape of a tsunami wave can serve as criteria for distinguishing a tsunami deposit from a storm deposit.

The general characteristics of tsunami deposits are described below based on some examples of ideal environments for deposition and preservation. Refers to tsunami deposits in the coastal lowlands, including shallow bays, lagoons and ponds. These areas, which are separated from the open sea, usually have sufficient water depth and accommodation space for the deposition of tsunami deposits with well-developed sediment structures. The relatively high sediment flux in this shallow water area provides favorable preservation conditions for fast burial of tsunami deposits (Fujiwara, 2008).

Tsunami deposits exhibit a wide spectrum of bed forms and sedimentary structures, which are related to the physical properties of the flow, such as velocity, density, viscosity, and predominant grain size. However, some general characteristics are recognized in the tsunami deposits from various deposition sites. This results from the fact that tsunamis have much longer wavelengths and periods than wind-generated waves, such as storm surges.

These extraordinary physical properties of the tsunami, under ideal conditions of deposition and preservation, are well recorded in the tsunami deposits as a unique arrangement pattern of bed forms and sedimentary structures: (1) alternation of sediment sheets deposited from high-energy sediment flows and silt beds, (2) repeated course reversals and (3) series of thinning and smoothing of sediment sheets.

Thick tsunami deposits sometimes consist of complete four deposition units, Tna to Tnd in ascending order (Figure 4A), which reflect the change in wave amplitude with time (Figure 4B). The Tna unit corresponds to relatively small waves in the early stages of a tsunami. At this stage, the sediment is fine grained with rip up clasts, which are bounded by mud drape. The very coarse-grained TnB unit is evidence of the occurrence of large waves in the middle of a tsunami. At this stage, the deposited sediment is a coarse grained dune with gravel fragments and anti-dune structures. The sequence of decimation and upward decimation from Tnb Unit to Tnc Unit shows the process of tsunami receding with a hummocky structure. The Tnd unit is a muddy layer with plant remains, formed by suspension fallout, indicates a return to a low-energy state after the tsunami (Fujiwara, 2008).

Tsunami deposits usually have a gradual bedding, fining upward and thinning landward sedimentary structure. Meanwhile, coastal sediments are characterized by repeated layers, containing a mixture of fragments originating from various sources, including cliff erosion, rivers, volcanoes, coral reefs, sea shells, sea level rise, and cannibalism of ancient coastal deposits (Trenhaile, 2005).

METHODS

The paleotsunami and paleosoil sediment samples were taken from Ternate Island on November 2022.

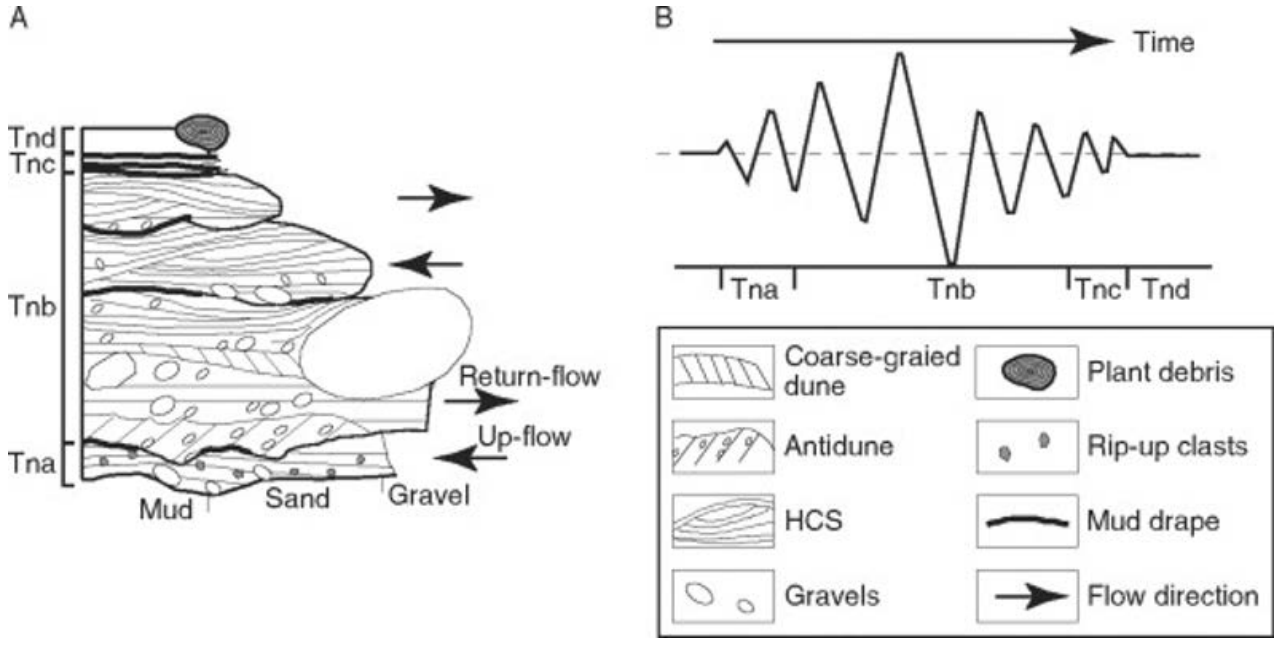

Figure 4. Sequence of tsunami deposits (Fujiwara, 2008)

Laboratory tests have been carried out for each sample, both paleotsunami and ancients coastal deposits, totally 12 samples by using the method grain size analysis.

Distribution of a sediment is the result of processes and infer the energy present (Heinzel, 2016), it can show the sediment transport itself, which can be read based on grain size tests in the laboratory. Grain size testing (granulometric) is carried out in the following stages:

1. Weigh the sample to determine the initial weight (wet condition)
2. Prepare each sample for drying
3. Removing the water content of the sample by drying the sample in the oven
4. Weigh the sample to determine the dry weight (Figure 5)
5. Determine the weight of the sample to be tested (analyzed)
6. Prepare the sieving equipment with the sieve assembly according to the desired opening sequence in phi units (-2.00; -1.00; 0.00; 1.00; 2.00; 3.00; 4.00; 5.00; and 6.00)
7. Sieve each sample so that the number of grains on each sieve size is obtained.
8. Weigh the sieve results with each sieve size (Figure 6).
9. The amount obtained is used as input for calculating and analyzing grain size using a statistical program, to determine its characteristics and deposition process.

After megascopic observations and conducting laboratory tests, the results obtained are used as input in a statistical calculation program. In this case we use the Excel program developed by Balsilllie (2002) and Blott & Pye (2001). As for the identification of grain size textures, we used literature materials obtained from online lectures by Prof. Meor Akif from the University of Malaya (2021), Dr. C.E. Heinzel from University of Northern Iowa (2016), and Mclaren (1980).

Mean

Graphic Mean can be calculated with formula from Folk and Ward, 1957 (Figure 7).

$$M = \frac{\emptyset 16 + \emptyset 50 + \emptyset 84}{3} \quad \ldots\ldots\ldots\ldots\ldots\ldots\ldots\ldots (1)$$

Sorting

Sorting measure of the range grain size present, apart from being visually observe (hand lens, microscope), also can be calculate from the result. Sorting is inclusive graphic standard deviation (σ_i). One standard deviation

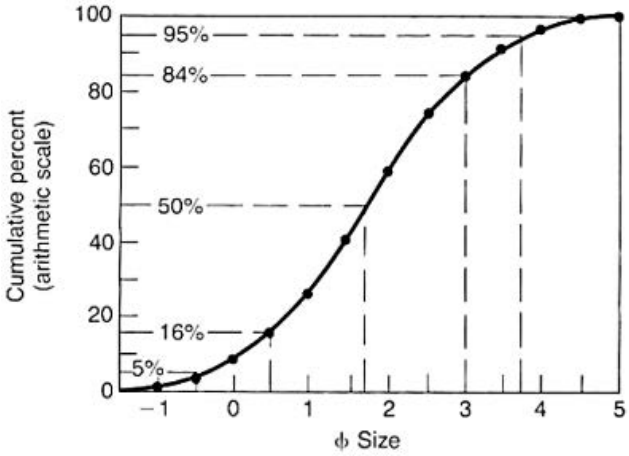

Figure 7. Determining the Graphic Mean Particle Size (Folk and Ward, 1957)

covers approximately the central 68% of area under

Figure 5. Weighing of the sediment samples

Figure 6. Drying (left) and Sieving (right) Machines

frequency curve (Figure 8), and can be calculated from grain size data (e.g. from sieve analysis), using the formula:

$$\sigma i = \frac{\emptyset 84 - \emptyset 16}{4} + \frac{\emptyset 95 - \emptyset 5}{6.6} \quad \ldots\ldots\ldots\ldots\ldots\ldots\ldots\ldots\ldots\ldots (2)$$

Illustration of sorting (Figure 9), corresponding to verbal terms and graphic standard deviation (Jerram, 2001):

Skewness

Skewness is a measure of the amount of deviation from a normal distribution (i.e., an asymmetrical frequency curve). Most of natural sediments do not yield a perfect normal grain size distribution (bell curve). Skewed distribution is asymmetrical distribution. Skewness can be calculated using formula:

Higher deviation from zero is greater skewness

Sorting Description	**Standar Deviation**
Very well sorted	< 0.35Ø
Well sorted	0.35 – 0.50Ø
Moderately well sorted	0.50 – 0.71Ø
Moderately sorted	0.71 – 1.00Ø
Poorly sorted	1.00 – 2.00Ø
Very poorly sorted	2.00 – 4.00Ø
Extremely Poorly Sorted	>4.00Ø

Kurtosis

Kurtosis is sharpness of a grain size frequency curve. Sharp-peaked (leptokurtic) better sorting in central portion

$$S = \frac{\emptyset 84 + \emptyset 16 - 2(\emptyset 50)}{2(\emptyset 84 - \emptyset 16)} + \frac{\emptyset 95 + \emptyset 5 - 2(\emptyset 50)}{2(\emptyset 95 - \emptyset 5)} \quad \ldots\ldots\ldots\ldots\ldots (3)$$

Calculated Skewness	**Verbal Skewness**
> + 0.30	Strongly Fine Skewed
+ 0.30 to + 0.10	Fine Skewed
+ 0.10 to – 0.10	Nearly Symetrical
- 0.10 to – 0.30	Coarse Skewed
<- 0.30	Strongly Coarse Skewed

(Figure 10). Flat-peaked (platycurtic) poorer sorting in central portion. Kurtosis can be calculated with the formula:

$$K = \frac{\emptyset 95 - \emptyset 5}{2.44(\emptyset 75 - \emptyset 25)} \quad \ldots\ldots\ldots\ldots\ldots\ldots\ldots\ldots\ldots\ldots (4)$$

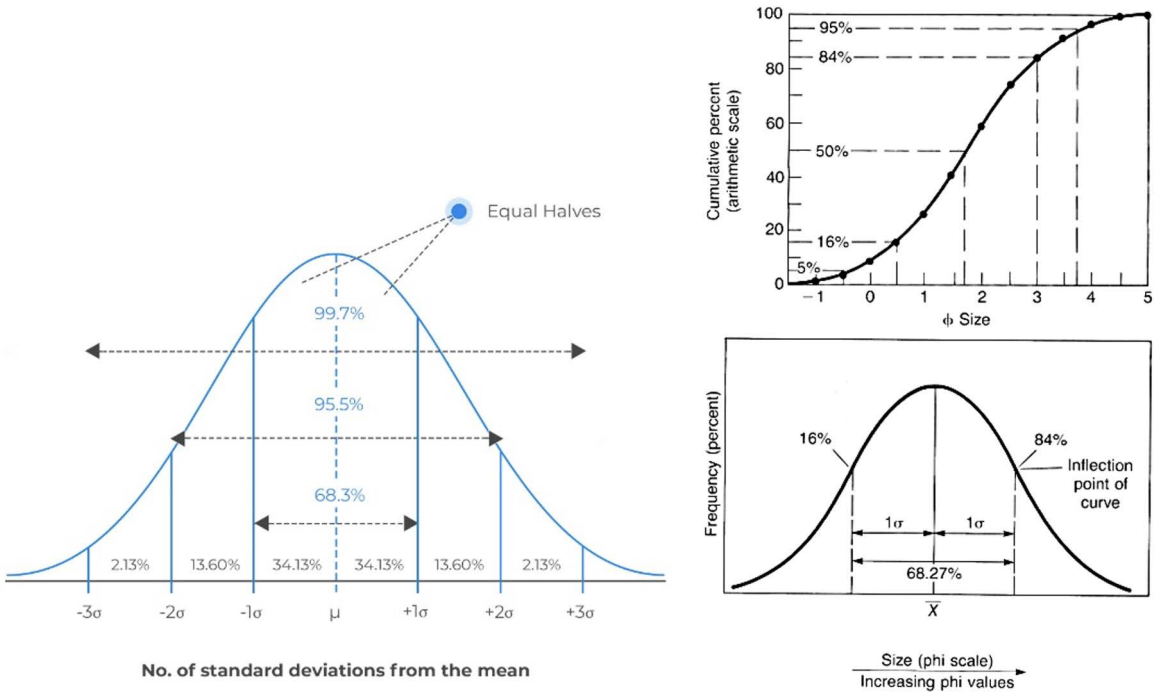

Figure 8. Graphical method of calculating sorting (Folk and Ward, 1957).

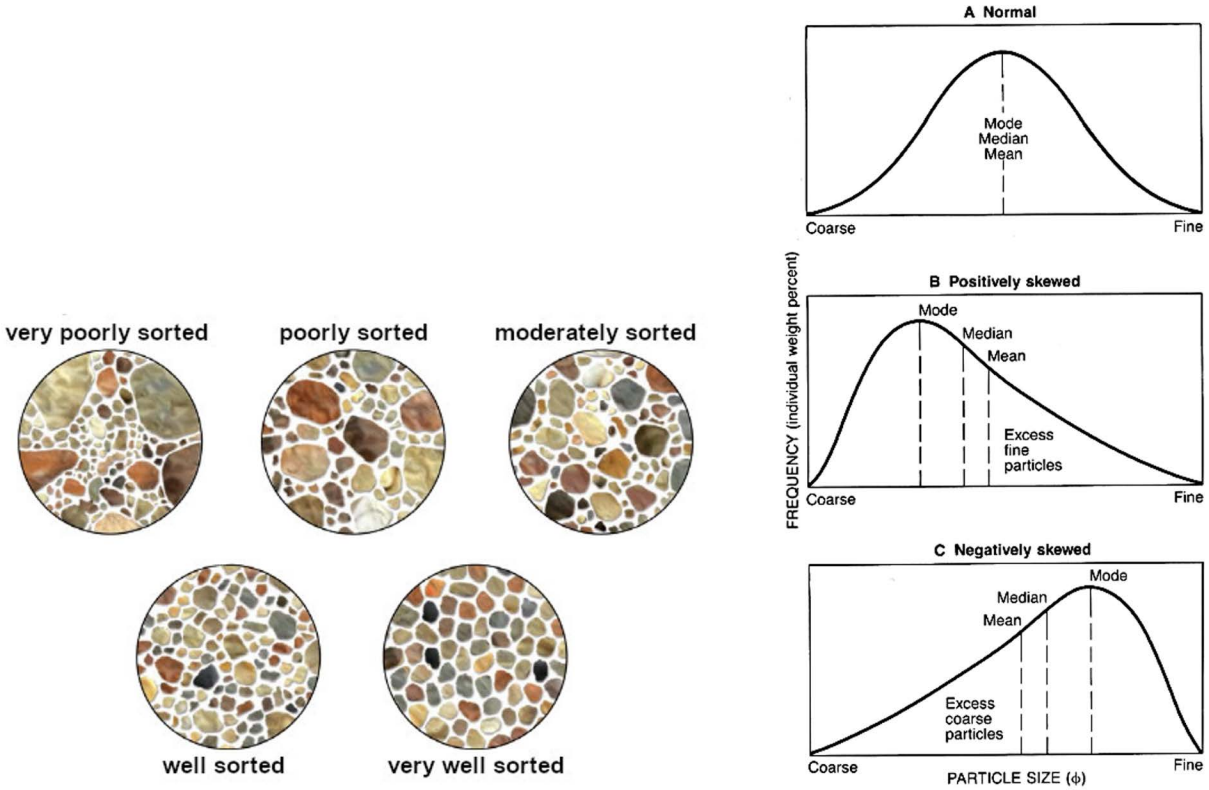

Figure 9. Illustration of Sorting (left) and Graphical Estimation of Skewness (right) (Geocache, 2023)

RESULTS AND DISCUSSION

The paleotsunami candidates were found at location of 127.29488°E – 0.82129°S. The youngest was deposited beneath the Gamalama eruption product which is occurred

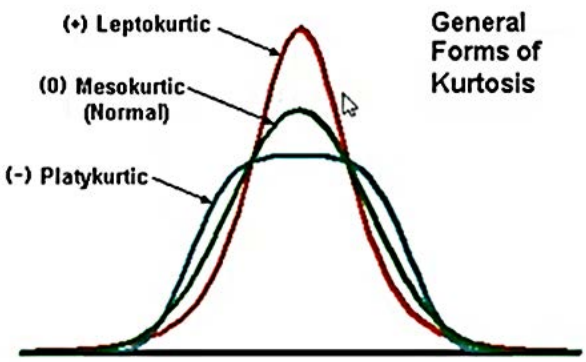

Figure 10. Graphic Estimation of Kurtosis (Akif, 2021)

Calculated Kurtosis	Verbal Kurtosis
< 0.67	Very Platykurtic
0.67 - 0.90	Platykurtic
0.90 - 1.11	Mesokurtic
1.11 - 1.50	Leptokurtic
1.50 - 3.00	Very Leptokurtic
>3.00	Extremely Leptokurtic

in 1907 (Figure 11). The thickness of the product of the Gamalama Volcano eruption reaches 7.3 m, with a distance of approximately 50 m from the coastline.

The first paleotsunami layer (J in Figure 11) is covered unconformably by paleosoil in the form of blackish coarse sand with a thickness of 5 cm, while below the layer it is bounded by paleosoil with a thickness of 15 cm, in the form of blackish gray old beach sand with rock fragments that have oriented nearly north-south or in the direction of the outcrop.

The first layer can be divided into three main layers, but there are very thin layers (mud drape) that separates the second layer from the first and the second to the third layers which has each thickness about 0,5 mm. The three main layers can be named as bottom (Tna) with thickness of 0.5 cm, middle (Tnb) of 2 cm, and top (Tnc) of 0.3 cm. The Tnd unit was very thin, so it can not easy to distinguish (Figure 12).

After excavating vertically downwards, it was found layers presumed to be older paleotsunami deposits with a thickness of 1.8 cm (Figure 11), which based on the difference in color, can be divided into two layers with an upper layer of 1 cm thick in the form of very fine sand with a light greenish gray color and 0.8 cm in the form of very fine brownish-gray sand. The second paleotsunami deposit was found under a 15 cm thick paleosoil. Layers suspected as the third paleotsunami deposit were found 15 cm later, as well as the fourth paleotsunami deposit with a thickness of 1.5 cm each. The layer which is suspected as the fifth or oldest paleotsunami deposit, was found 20 cm after the fourth layer, with a deposit thickness of 5.5 cm.

Let us named the youngest paleotsunami deposit as the first (1st), the next paleotsunami deposit which is older than the first one, we called the second (2^{nd}), the third (3^{rd}), the Forth (4^{th}) and the fifth (5^{th}) paleotsunami deposits. Only three samples of tsunami sediments could analysed in the laboratory, which are the first, the second and the fifth. While the third and the forth could not be taken for analysed because they were too thin, so they were mixed with the paleosoil above and below them. Here is the respective weight for granulometrical analysis (Table 2).

Megascopically, it was observed the physical properties of the sediment grains of the paleotsunami deposits which are then calculated statistically. Below (Figure 13) are the first, second, and the fifth paleotsunami sediment grains. It can be seen here that the grain color is dominated by dark gray and black, and part of it is silicate in the form of transparent quartz, red and yellowish white rocks.

Based on statistics calculation of grain-size distribution, it is obtained values of mean grain size, sorting, skewness and kurtosis (Table 3). The results obtained show that the sorting of all paleotsunamis were poorly sorted, those indicate the sediment size are mixed (large variance), and this is due to the energy of tsunami wave is varies in time when transport and deposits the sediment.

Skewness varied from strongly fine skewness to strongly coarse skewness, indicating of prevailing changing of tsunami wave energy from very high when its run up inland decreasing when it returning into the sea. Negative skewness shown by top layer of the 1^{st} paleotsunami deposits and middle layer of the 5^{th} paleotsunami deposits indicate of finer grain sizes. While positive values show coarser grain.

Kurtosis of the first top layer is leptokurtic, means the frequency distribution or its graphical interpretation having greater kurtosis than normal distribution or fat-tailed, meaning of having many outliers, while middle and bottom are platykurtic distribution which mean thin tailed, or have few outliers. The fifth top and middle layer both have mesokurtic, which mean the outlier characteristic of an extreme event.

Based on the results of granulometric analysis, information was obtained that the first paleotsunami (the youngest) was dominated by coarse silt (fine-sized sediment). In the top of the first paleotsunami, has composition of fine grains dominates over coarse grains

(silt 56.84%; sand 42.8417% and gravel 0.32%) and containing roots remains. The middle part of paleotsunami first layer has the percentage of sand-sized grains is slightly more than fine grains (silt 45.7013%; sand

Figure 11. Left: Paleotsunami deposits found beneath the product of the Gamalama volcano; Right: Outcrop with five layers of suspected paleotsunami deposits (B,D,F,H and J) bounded by paleosoil (A, C, E, G, I and K)

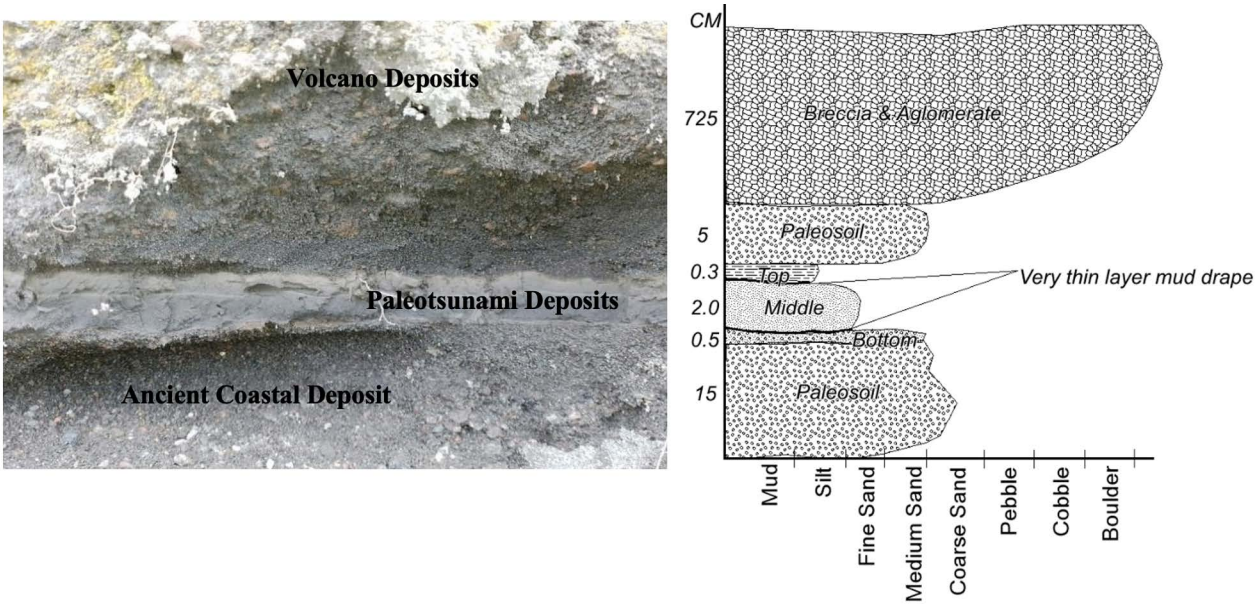

Figure 12. The Youngest First Layer Beneath the Product of the Gamalama Volcano (left) and Its Profil (right)

Table 2. The Analyzed Tsunami Suspects Samples

No.	Name of Samples	Weight (Gram)	
		Wet	Dry
1.	The first Paleotsunami (*top*)	202.32	147.61
2.	The first Paleotsunami (*middle*)	208.73	163.25
3.	The first Paleotsunami (*bottom*)	278.61	237.08
4.	The second Paleotsunami	33.08	29.17
5.	The fifth Paleotsunami (*top*)	24.50	21.26
6.	The fifth Paleotsunami (*middle*)	81.07	67.60
7.	The fifth Paleotsunami (*bottom*)	107.36	90.90

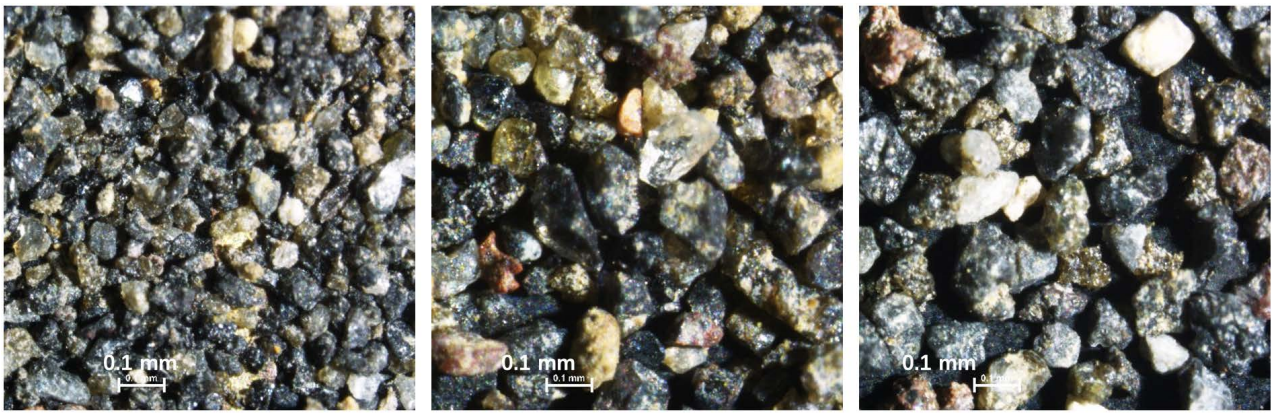

Figure 13. Megascopically of first Paleotsunami (left), the second (middle) and the fifth paleotsunami deposits (right)

Table 3. Sediment Texture of Mean, Sorting, Skewness and Kurtosis

Name of Paleotsunami	Mean	Sorting	Verbal of Sorting	Skewness	Verbal of Skewness	Kurtosis	Verbal of Kurtosis
1st paleotsunami (Top)	3.17	1.10	Poorly Sorted	-0.56	Strongly Coarse Skewed	1.37	Leptokurtic
1st paleotsunami (Middle)	2.58	1.36	Poorly Sorted	0.46	Strongly Fine Skewed	0.78	Platykurtic
1st paleotsunami (Bottom)	0.83	1.28	Poorly Sorted	0.30	Fine Skewed	0.72	Platykurtic
2nd paleotsunami	1.20	1.03	Poorly Sorted	1.33	Strongly Fine Skewed	0.63	Very Platykurtic
5th paleotsunami (Top)	1.43	1.47	Poorly Sorted	0.08	Nearly Symmetrical	0.97	Mesokurtic
5th paleotsunami (Middle)	1.92	1.58	Poorly Sorted	-0.24	Coarse Skewed	0.92	Mesokurtic
5th paleotsunami (Bottom)	1.17	1.63	Poorly Sorted	0.12	Fine Skewed	0.82	Platykurtic

Table 4. Percentage of grain size in paleotsunami and paleosoil deposits

No.	Name of Layers	% Gravel-Pebble	% Sand	% Silt
1.	The 1st Paleotsunami (Top)	0.32	42.84	56.84
2.	The 1st Paleotsunami (Middle)	0.85	53.45	45.70
3.	The 1st Paleotsunami (Bottom)	4.47	52.28	43.26
4.	The 2nd Paleotsunami	0.65	91.70	7.65
5.	The 5th Paleotsunami (Top)	1.98	86.12	11.90
6.	The 5th Paleotsunami (Middle)	2.01	80.16	17.83
7.	The 5th Paleotsunami (Bottom)	3.61	83.63	12.75

53.4512%; gravel 0.8475%). Meanwhile the bottom of first paleotsunami layer, has coarse size grains greater than finer grains and has more gravel (silt 43.26%; sand 52.28%; gravel 4.47%). The results are as listed in Table 4.

The following is a histogram that shown by the first (the youngest) paleotsunami deposits suspect. Figure 14 is the histogram of the bottom layer, shows dominantly percentage of sand, the existence of gravel, and a bimodal curve indicating that the sediment sources come from two different places.

The results of the grain size analysis were entered into the Excel program developed by Basillie et al. (2002), which plotted grain size of phi units in X directions and Cummulative Percent in Y directions, in order to determine the agencies of transportation and depositional process (Figure 15). Below is the guide how to read the curves.

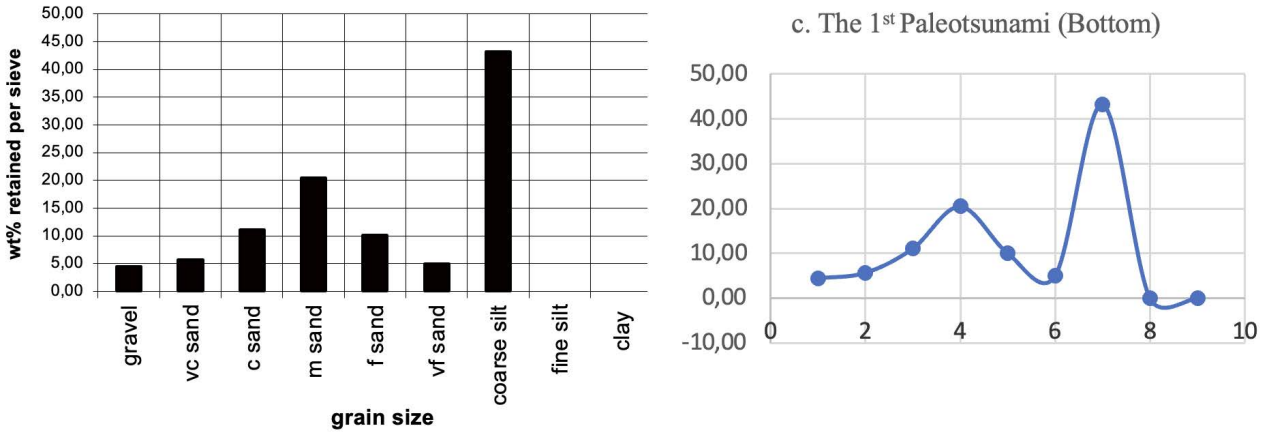

Figure 14. The bottom layer of First Paleotsunami sediment histogram (left) and Grain size curve showing sediment sources two different sources bimodial in the Bottom layer of youngest (the first) paleotsunami deposits (right)

Basic line-segment geometries identifying transportation and depositional signatures forthcoming from the use of aritmethic probability paper. Line-segment geometries were determined by Tanner (1986, 1991) and Balsillie, 1995 (Balsillie, 2002).

Figure 16 is an accumulation plot, shows the deposition process of the bottom layer, which has steep sloping indicates highest energy of the deposition characterized by deposition of pebble and coarse-sized grains (D). The character shown by the bottom layer shows the mechanism of sediment deposition by the tsunami waves when run up inland.

Next is the histogram of middle layer of first paleotsunami deposits (Figure 17), which shows of gradually large numbers from coarser to the finer sediment grains and unimodal curve indicating of single source of sediment.

Figure 18, is the deposition process of the middle layer, which begins with tsunami wave activity, and is deposited by sand by low to moderate wave energy levels and deposits coarse sand-sized material (B). This condition is continued with the fluvial energy phase, with the energy level being higher than before indicating that there are wave currents that will return seaward and deposits finer sized grains (D).

The histogram of the top layer of the first paleotsunami deposits, which shows the predominance of fine grains, indicating that the suspension process played a more important role, this occurred when the tsunami energy was exhausted and receded back towards the sea, while the percentage curve shows unimodal indicating of the single source of sediment (Figure 19).

The deposition process of the top layer of first paleotsunami deposits, beginning with the flow of tsunami waves with moderate to high energy and depositing sand-sized grains (D), followed by the process of decreasing the energy level to be lower, and depositing finer grains (G),

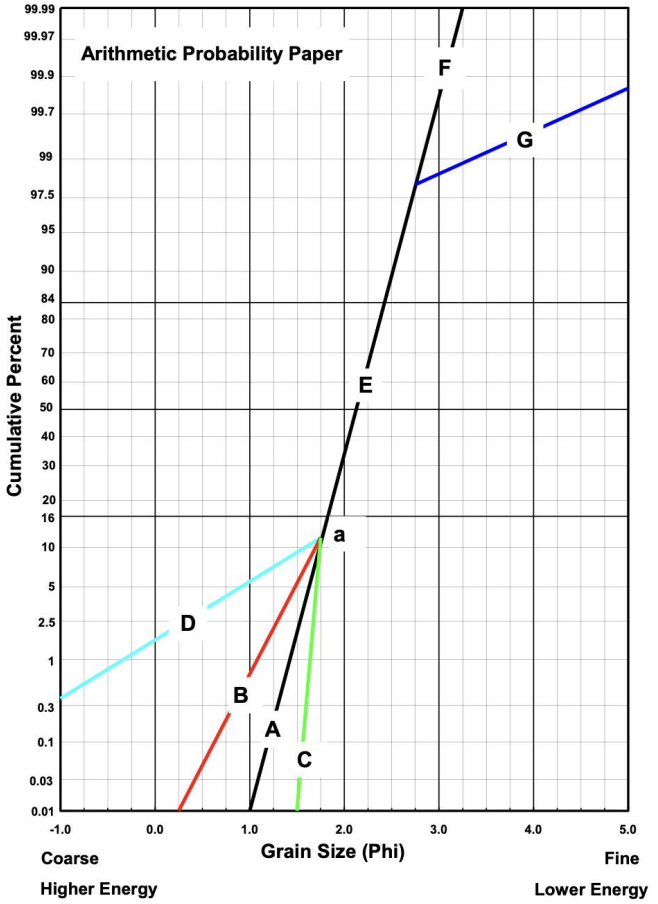

Figure 15. Geometry of the basic line segments that identify trans-deposition processes (Tanner, 1986, 1991; Balsillie, 1995; in Balsillie, 2002)

which signifies settling current from the water, but continue with the moderate energy (D) (Figure 20).

The second paleotsunami deposit or older than the first paleotsunami deposit, showing coarse grains predominate over fine grains (Table 2), with the depositional process showing segment B initiating wave activity with highest energy and depositing very coarse

Table 5. Guide of the Determination of Transpo-Depositional Agencies (Balsillie, 1995)

Segment	Descrition of Granulometric Interpretation
---AEF---	Gaussian distribution. Plot as a straight line on probability paper.
---B---	Shows that the element of the transo-deposition force operating is wave activity; point relative to segment E is termed a surf break. This relatively gentle slope represents beach sand. The higher the slope of segment B, the higher the wave energy. Note that for sand-sized materials, breaking waves usually occur for low to moderate wave energy conditions. For high-energy waves, point a moves from the plot (towards the bottom) and segment B disappears (that is, the energy of the wave exceeds the strength of even the coarsest available sand (Savage, 1958; Balsilie, 1999).
---C---	Shows eolian process; point a is termed, relative to segment B, the eolian hump.
---D---	Represents fluvial energy; has a steep slope. The greater the slope, the higher the energy level. This segment is called the fluvial rough tail. It may also represent a transpo-depositional tidal current process.
---E---	The middle segment of the sample distribution
---G---	Represents a low-energy tail which is called a regulatory tail and, if present, may indicate a decrease in energy for the total distribution or for segments of the distribution containing coarser sediments. This indicates settling from water.

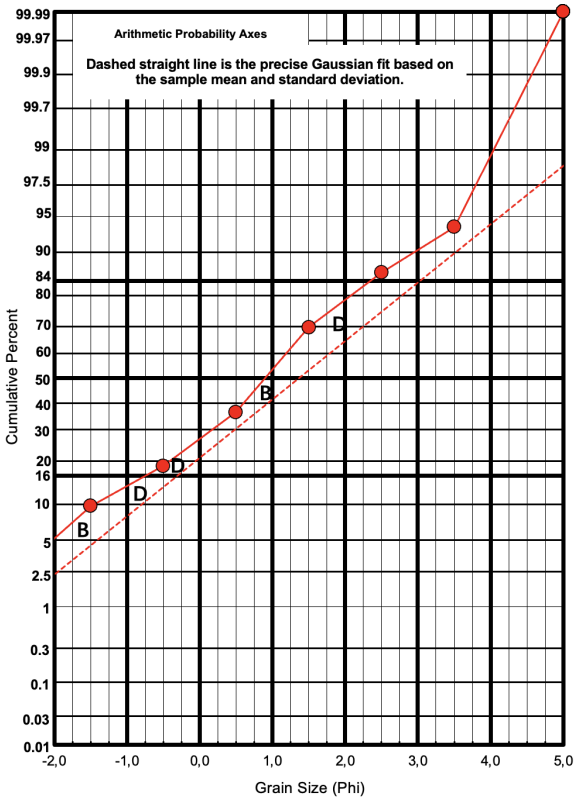

Figure 16. The bottom layer of first paleotsunami deposition process diagram.

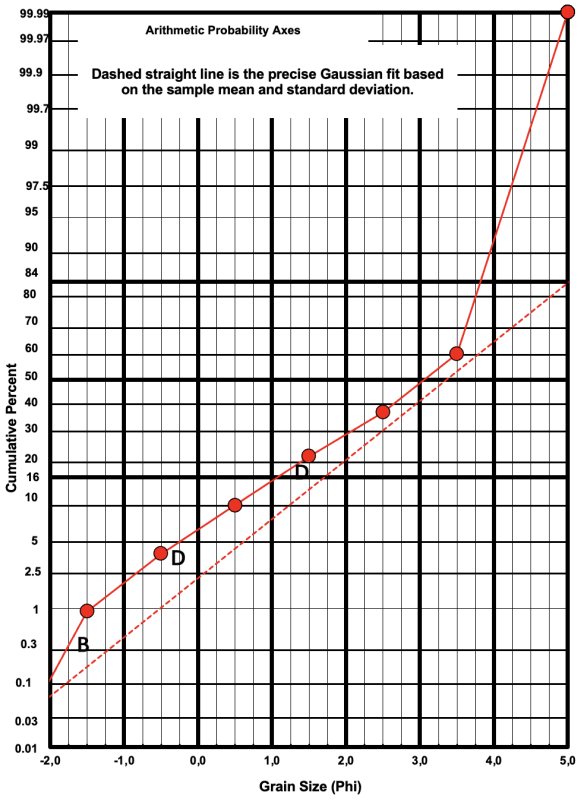

Figure 18. The middle layer of first paleotsunami deposition process diagram

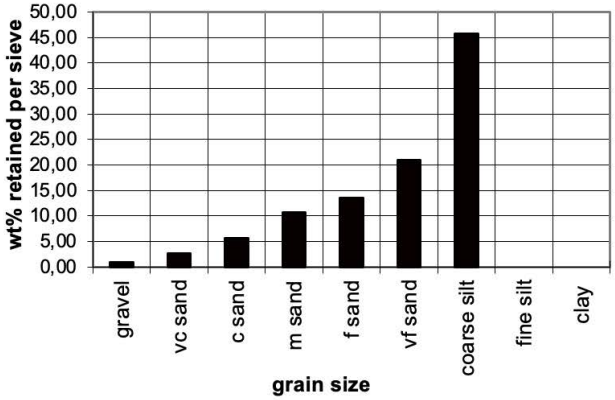

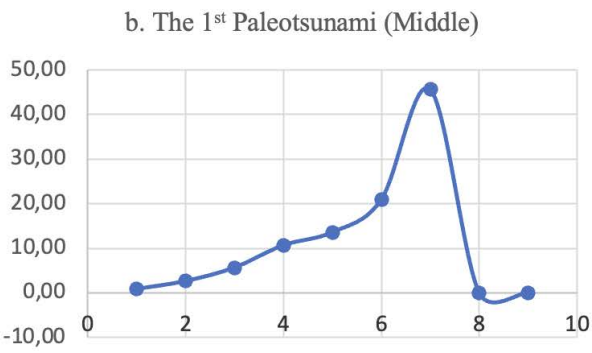

Figure 17. The middle layer of First Paleotsunami sediment histogram (left) and Grain size curve showing unimodal of single sediment source.

sand-sized material, followed by processes transpo-

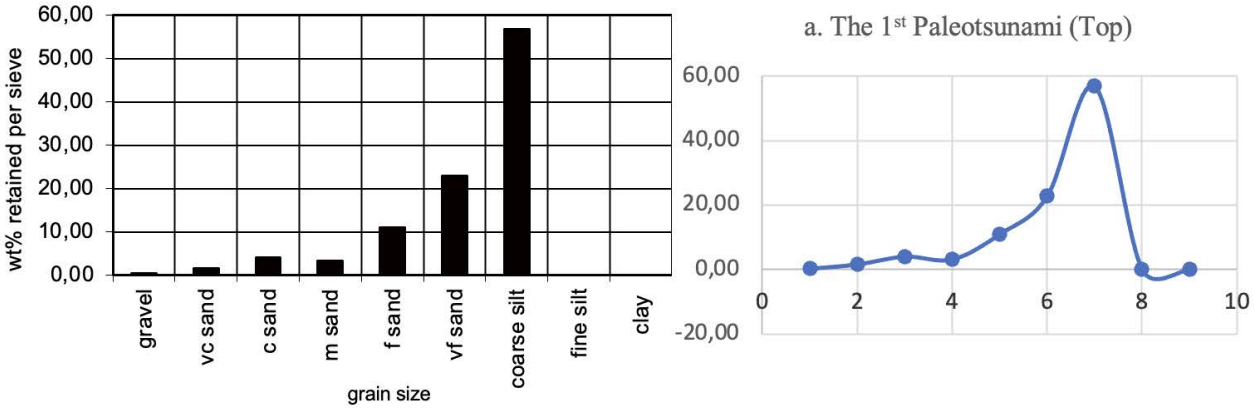

Figure 19. The First Paleotsunami sediment histogram at the top (left) and Grain size curve showing unimodal of single sediment source (right).

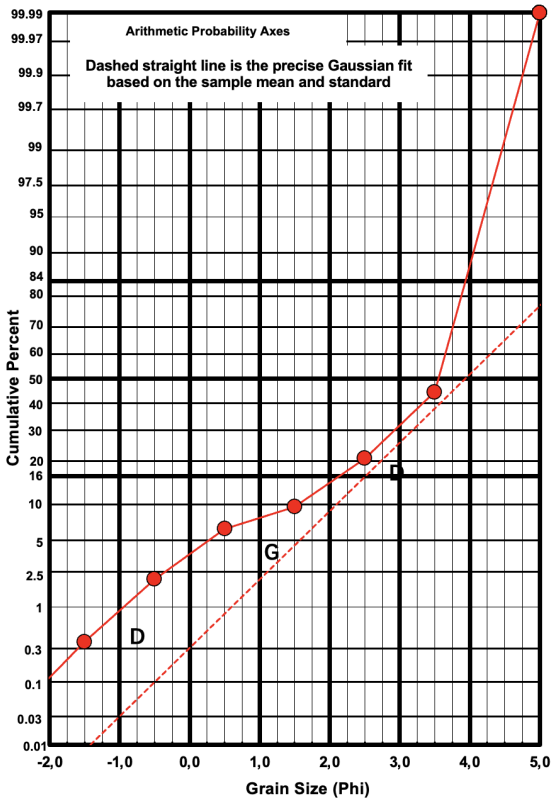

Figure 20. The Top Layer of the first paleotsunami deposition process diagram (Top)

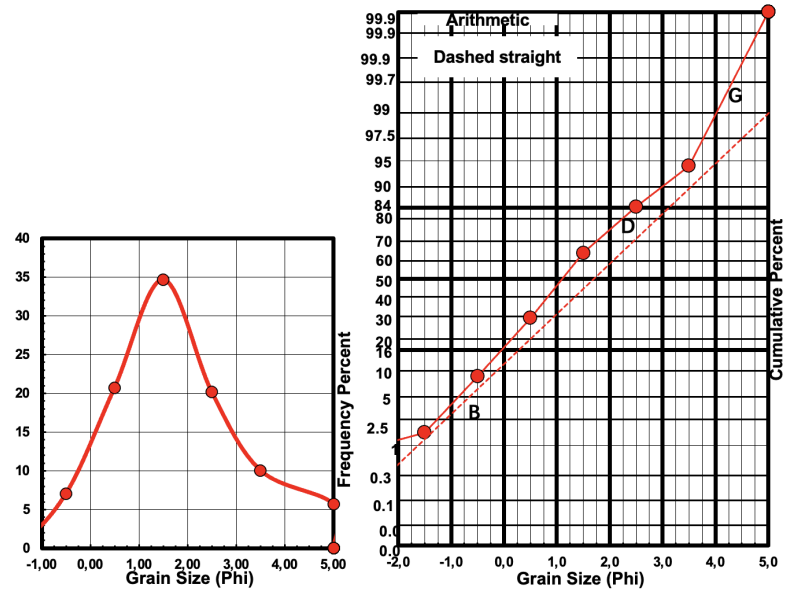

Figure 21. The Top Layer of the second paleotsunami deposition process diagram (Top)

depositional of tidal currents (segment D) with high energy levels and deposits coarse-sized grains (Figure 21).

The fifth paleotsunami deposit has the same characteristics as the second paleotsunami deposit, which begins with segment B followed by segment D which shows high depositional energy and deposits coarse-sized material (Figure 22).

Both the second and fifth paleotsunami deposits do not have fine grain layers, this is probably due to the very thin thickness of the layers so that they were not properly detected during laboratory testing.

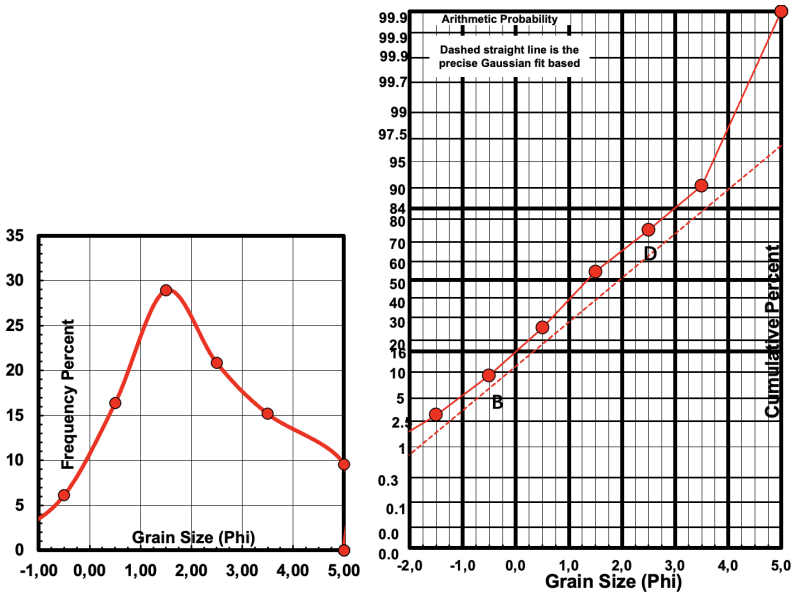

Figure 22. The Top Layer of the fifth paleotsunami deposition process diagram (Top)

CONCLUSSIONS

According to those granulometric analysis, it shows that the deposition of the youngest paleotsunami deposits was initiated by a very strong current with the greatest energy, so that it deposited a very coarse sand grains down to gravel. Followed by a gradual decrease in energy and the process of the tsunami wave starting to reverse direction towards the sea, and then receding with the lowest energy and depositing finer grains. While the sediment sources come from two different places, indicating the source comes from both the sea and the coast around the place where the paleotsunami deposits were deposited.

The vertical changes in the grain size distribution and in the type of sedimentary structures in the youngest paleotsunami deposits are clarified. The paleotsunami deposits are mainly composed of four units (Tna, Tnb, Tnc and Tnd in ascending order). The Tnd unit or the upper part of the youngest paleotsunami deposits contain the remains of plant roots, which shows the characteristics of tsunami deposits.

Variations in the mean, sorting, skewness and kurtosis values indicate a change in the energy of the tsunami wave, causing a change in grain size.

ACKNOWLEDGEMENTS

The author would like to express deep gratitude to the Volcanology and Geological Hazard Mitigation, Geology Agency, Ministry of Energy and Mineral Resources, Ternate Island Tsunami Deposit Investigation Team, all officers at the Gamalama Volcano Observation Post, in Ternate, Indonesian Navy Base in Ternate, STKIP Kie Raha Ternate, and all parties who are very helpful for the smooth running of activities that cannot be mentioned one by one.

REFERENCES

Akif., M., 2021. *Online Lecture of Sedimen Lecture, Texture: Grain Sorting.* Sedimentology Lecture 2, Texture: Grain Sorting - YouTube

Balsillie, J.H., 1995. *William F. Tanner on Evironmental Clastic Granulometry: Florida Geological Survey*, Special Publication No. 40, 144 p.

Balsillie, J.H., Donoghue, J.F., Butler, K.M., and Koch, J.L., 2002. Plotting equation for Gaussian, percentiles and a spreadsheet program for generating probability plots. Journal of Sedimentary Research, 72 (6), p. 929-933.

Blott, S.J. and Pye, K., 2001. *GRADISTAT: a Grain Size Distribution and Statistics Package for the Analysis of Unconsolidated Sediments*. Earth Surface Processes and Landforms 26, 1237-1248.

Bronto, S., Hadisantono, R.D., Lockwood, J.P., 1982. *Peta Geologi Gunung Api Gamalama, Ternate, Maluku Utara*. Direktorat Vulkanologi, Departemen Energi dan Sumber Daya Mineral.

Folk, R.L., and Ward, W.C., 1957. *A Study in the Significance of Grain-Size Parameters. Journal of Sedimentary Petrology,* 27, 3-26. https://doi.org/10.1306/74D70646-2B21-11D7-8648000102C1865D

Fujiwara, O., 2008. *Tsunami Depositional Processes Reflecting the Waveform in a Small Bay Interpretation from the Grain-Size Distribution and Sedimentary Structures*. In Book: Tsunamiites pp. 133-152

Geocache, 2023. Urban earth - *Sediment Sculptor*. https://www.geocaching.com/geocache/GC7Z2X2

Google Earth, 2022. *Ternate Island*. Online Application.

Haris, Ron., dan Major, J., 2016. *Waves of destruction in the East Indies: the Wichmann catalogue of earthquakes and tsunami in the Indonesian region from 1538 to 1877*. Geological Society Publication. https://www.lyellcollection.org/journal/sp

Heinzel, C.E., 2016. *Particle-Size Analysis*. Online Presentation. Dept. of Earth and Environmental Science, University of Iowa.

Jerram, D.A., 2001. *Visual Comparator for Degree of Grain-Size Sorting in Two and Three Dimensions*. Computers and Geosciences 27 (4): 485-492. http://doi.org/10.1016/S0098-3004(00)00077-7

McLaren, P., 1980. *An Interpretation of Trends in Grain Size Measures*. Geological Survey of Canada.

Rachman, G., Santosa, B.J., Nugraha, A.D., Rohadi, S., Rosalia, S., Zulfakriza, Sungkono, Sahara, D.P., Muttaqy, F., Supendi, P., Ramdhan, M., Ardianto, Afif, H., 2002. *Seismic Structure Beneath the Molucca Sea Collision Zone from Travel Time Tomography based on Local and Regional BMKG Networks*. Appl. Sci. 2022, 12(20), 10520; https://doi.org/10.3390/app122010520

Satake, K., and Imamura, F., 1995. *Tsunami in Ternate Island*. In Latief et al., 2000, Tsunami Catalog.

Soloviev, S.L., dan Go., Ch. N., 1974. *Tsunamis on the Western Shore of the Pasific Ocean*. Moscow, "Nauca" Publishing House, 308 Halaman.

Tanner, W.F., 1986. *Inherited and Mixed Traits in The Grain Size Distribution*: In W.F. Tanner (ed.), Modern Coastal Sediments and Processes, Proceedings of the 9th Symposium on Coastal Sedimentology Tallahassee, FL: Department of Geology, Florida State University, p. 41-50.

Tanner, W.F., 1991. *Suite Statistics: the Hydrodynamic Evolution of the Sediment Pool*: In J.P.M. Syvitski (ed.) Principals and Application of Particle Size Analysis, Cambridge: Cambridge University Press, p 225-236.

Trenhaile, A.S., 2005. *Beach Sediment Characteristics*. In Schwartz, M.L., (eds) Encyclopedia of coastal

science. Encyclopedia of Earth Science Series. Springer, Dordrecht. pp 177-179. https://doi.org/10.10071/1-4020-3880-1_41